OPTICAL COMMUNICATION

PACS numbers: 42.79.Sz; 42.81.Dp
DOI: 10.1070/QE2007v037n09ABEH013470

Study of new modulation data-transmission formats for dispersion-controlled high-bit-rate fibreoptic communication lines

O.V. Shtyrina, M.P. Fedoruk, S.K. Turitsyn

***Abstract*. The results of simulation of the propagation of optical signals in a multichannel high-bit-rate fibreoptic communication line with a combined scheme for amplifying optical signals based on new modulation data-transmission formats are presented. A comparative characteristic of formats with the amplitude and phase modulations of the electromagnetic-wave carrier is presented. The results of numerical simulation show that phase-modulation formats have a considerable advantage over amplitude formats. The use of phase-modulation formats leads to an increase in the maximum range of high-quality communications by a factor of three on average compared to amplitude-modulation formats. It is shown that optimal propagation regimes both in the case of amplitude-modulation and phase-modulation formats are realised for the normal (negative) group-velocity dispersion. However, the dispersion value for amplitude-modulation formats proves to be considerably greater than for phase-modulation formats.**

Keywords: *fibreoptic communication lines, modulation data-transmission formats, mathematical simulation.*

1. Introduction

The transmission capacity (total data-transmission rate) of modern multichannel fibreoptic communication lines (FOCLs) can be further increased by expanding the spectral range $\Delta\nu$ and increasing the spectral efficiency γ of data transmission.

Consider a multichannel FOCL with the data-transmission rate B in one frequency channel and the distance $\Delta\nu$ between adjacent frequency channels. The spectral data-transmission efficiency is $\gamma = B/\delta\nu$ and the total data-transmission rate over all channels is $B_\Sigma = \gamma\Delta\nu$.

To expand considerably the spectral range $\Delta\nu$, an optical amplifier with a uniform gain band of width of several hundreds of nanometres is required [1]. Another possible and promising method is based on increasing the spectral data-transmission efficiency γ. Both these methods have their own advantages and disadvantages.

The spectral efficiency γ can be increased by increasing the transmission capacity B per frequency channel or decreasing the distance $\delta\nu$ between adjacent frequency channels. It was pointed out in [2] that the first way is economically more promising because, as follows from estimates, the increase in the data-transmission rate by four times reduces the cost of a transmitted bit approximately by a factor of 2.5. At the same time, the increase in the data-transmission rate is accompanied by distortions of digital signals in communication lines. In particular, distortions caused by chromatic dispersion increase proportionally to the square of the channel bit rate B^2, distortions caused by polarisation mode dispersion (PMD) are proportional in the first approximation to B, and the loss power is also proportional to B [2].

In this connection the study of new modulation data-transmission formats, which would be less sensitive to dispersion and nonlinear distortions in high-bit-rate communication lines ($B = 40$ Gbit s^{-1} and higher) is of current interest.

In this paper, we compare several types of modulation data-transmission formats by the example of a dispersion-controlled FOCL (with the distributed dispersion). Dispersion-controlled systems use periodically alternating fibres with the opposite signs of chromatic dispersion, which allows one to control the dispersion broadening of a pulse, to increase the signal-to-noise ratio, and decrease the influence of nonlinear effects distorting optical pulses (see, for example, [3]). In particular, a periodic section of a dispersion-controlled FOCL shown in Fig. 1 consists of periodic sections containing a standard single-mode fibre

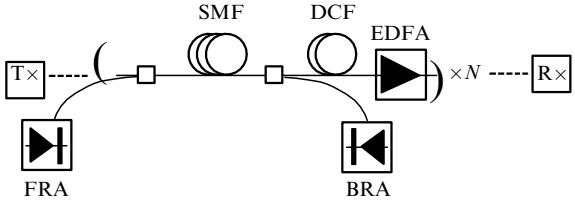

Figure 1. Schematic configuration of a fibreoptic communication line: (T) transmitter; (R) receiver; (EDFA) erbium-doped fibre amplifier; (FRA) forward-pumped Raman amplifier; (BRA) backward-pumped Raman amplifier; (SMF) standard single-mode fibre; (DCF) dispersion-compensating fibre.

O.V. Shtyrina, M.P. Fedoruk Institute of Computational Technologies, Siberian Branch, Russian Academy of Sciences, prosp. Akad. Lavrent'eva 6, 630090 Novosibirsk, Russia; e-mail: mife@ict.nsc.ru;
S.K. Turitsyn Institute of Automatics and Electrometry, Siberian Branch, Russian Academy of Sciences, prosp. Akad. Koptyuga 1, 630090 Novosibirsk, Russia; e-mail: s.k.turitsyn@aston.as.uk

Received 23 October 2006; revision received 20 March 2007
Kvantovaya Elektronika **37** (9) 885 – 890 (2007)
Translated by M.N. Sapozhnikov

(SMF) with the anomalous (positive) group-velocity dispersion and a dispersion-compensating fibre (DCF) with the normal (negative) dispersion. The high local chromatic dispersion of the FOCL reduces the influence of four-wave mixing in channels, while the low average chromatic dispersion of FOCL periodic section

$$\langle D\rangle = \frac{D_{\mathrm{SMF}}L_{\mathrm{SMF}} + D_{\mathrm{DCF}}L_{\mathrm{DCF}}}{L_{\mathrm{SMF}} + L_{\mathrm{DCF}}}$$

provides the suppression of random deviations of the time positions of optical signals. Here, D_{SMF} and L_{SMF} are the local chromatic dispersion and the SMF length, respectively, and D_{DCF} and L_{DCF} are these quantities for the DCF.

The SMF and DCF parameters used in calculations are presented below.

Single-mode fibre

Losses at 1550 nm/dB km^{-1}	0.20
Losses at 1455 nm/dB km^{-1}	0.25
Effective mode area/μm^2	80
Dispersion/ps nm^{-1} km^{-1}	17
Dispersion slope/ps nm^{-2} km^{-1}	0.07
Raman coefficient $g_{\mathrm{ps}}/A_{\mathrm{eff}}$/W^{-1} km^{-1}	0.42
Raman scattering coefficient ε_{p}/km^{-1}	7.05×10^{-5}
Rayleigh scattering coefficient ε_{s}/km^{-1}	5.4×10^{-5}
Nonlinear refractive index/m^2 W^{-1}	2.7×10^{-20}

Dispersion-compensating fibre

Losses at 1550 nm/dB km^{-1}	0.65
Effective mode area/μm^2	19
Dispersion/ps nm^{-1} km^{-1}	−100
Dispersion slope/ps nm^{-2} km^{-1}	−0.41
Nonlinear refractive index/m^2 W^{-1}	2.7×10^{-20}

Modulation data-transmission formats considered in our paper are shown schematically in Fig. 2. Let us characterise them briefly.

Formats presented in Figs 2a, b use the amplitude shift keying (ASK). A usual on–off binary format has two information power values corresponding to the on or off state of a transmitter (logic unity or zero). This format is called the RZ OOK (Return to Zero On–Off Keying) format in the literature; all elementary bits in it have the same phase (Fig. 2a). Another example of the amplitude format is $\pi/2$ AP RZ OOK ($\pi/2$ Alternate-Phase Return to Zero On–Off Keying) format, in which the phases of bits are successively alternated and take values 0 and $\pi/2$ (Fig. 2b) [4].

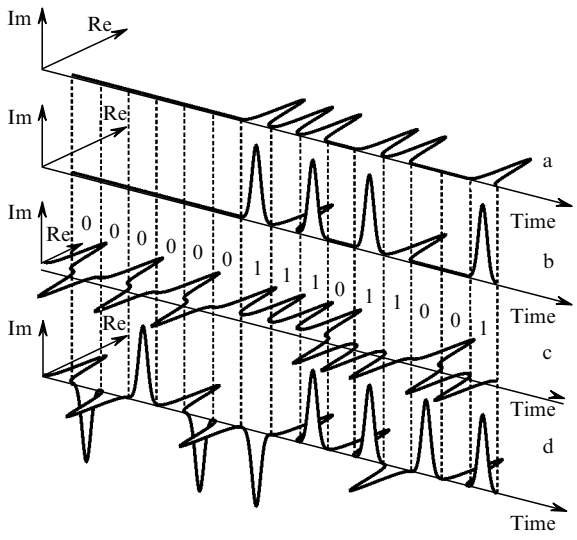

Figure 2. Schematic representation of different data-transmission modulation formats: RZ OOK format (a), $\pi/2$ AP RZ OOK format (b), RZ DPSK format (c), and $\pi/2$ RZ DPSDK format (d).

Formats presented in Figs 2c, d use the phase shift keying (PSK) to code information. In this case, one should bear in mind that optical communication lines considered in our paper use differential phase methods in all phase modulation formats when information is introduced into the relative shift of the optical phase of two successive pulses. Thus, in the usual return to zero differential phase-shift keying (RZ DPSK) format, the logic zero is coded when the optical-pulse phase in the bit interval is shifted by π with respect to the phase of the previous bit, while the logic unit corresponds to the same phases in two adjacent bits (Fig. 2c). In this case, the same power of the carrier pulse corresponds to all elementary bits.

It has been shown in a number of papers (see, for example, [5–8]) that this format considerably improves the quality of data transmission in optical communication systems compared to the usual digital OOK format. This is caused by three reasons. First, the method of balanced detection in the DPSK format reduces the bit error rate (BER) compared to the usual data-transmission format. Second, the DPSK format is considerably more stable with respect to the action of parasitic nonlinear effects on the optical signal, which appear due to phase cross-modulation. All bit intervals in this format are filled with optical pulses, and the power distribution among bits is uniform compared to the usual format. Third, a random phase shift of adjacent bits can reduce the efficiency of four-wave mixing. By decreasing the BER, it is possible to increase the distance between retranslators, to increase the communication range, and to increase the information capacity of the optical communication system.

The logic unity in the format shown in Fig. 2d is coded when the phase of an optical pulse is shifted by $\pi/2$ with respect to the phase of the previous bit, while the logic zero is coded when the phase is shifted by $-\pi/2$ [9]. This format was called the $\pi/2$ RZ DPSK format [9].

2. Mathematical formulation of the problem

The propagation of an optical signal along a FOCL is described by the generalised nonlinear Schrödinger equation for the complex envelope A of the electromagnetic-field amplitude [10]:

$$\mathrm{i}\frac{\partial A}{\partial z} + \mathrm{i}\gamma_{\mathrm{s}}A - \frac{\beta_2}{2}\frac{\partial^2 A}{\partial t^2} - \frac{\mathrm{i}\beta_3}{6}\frac{\partial^3 A}{\partial t^3} + \sigma\left[|A|^2 + \frac{\mathrm{i}}{\omega_0}\frac{\partial}{\partial t}\left(|A|^2 A\right) - T_{\mathrm{R}}A\frac{\partial |A|^2}{\partial t}\right] = 0. \qquad (1)$$

Here, z is the distance along the fibreoptic line; t is time; $|A|^2$ is the signal power; β_2 is the group-velocity dispersion parameter; β_3 is the third-order dispersion term; T_{R} is the Raman response time; σ is the Kerr nonlinearity coefficient; and γ_{s} is the effective coefficient taking into account the signal decay and amplification. The quantities β_2, β_3, σ, and γ_{s} are represented as functions of z to take into account

variations in these parameters on passing from one fibre type to another. The nonlinearity coefficient σ is defined by the expression

$$\sigma = \frac{2\pi n_2}{\lambda_0 A_{\text{eff}}},$$

where n_2 is the nonlinear refractive index; λ_0 is the carrier wavelength; $\omega_0 = 2\pi c/\lambda_0$; c is the speed of light; and A_{eff} is the effective area of the fibre mode. We solved Eqn (1) numerically by the method of splitting over physical processes (see, for example, [10]).

An important estimate of the 'quality' of a communication system is the BER, which is the ratio of the number of erroneous bits to the total number of transmitted bits [11]. The typical acceptable BER value is 10^{-9}. It is obvious that such a small BER cannot be directly simulated, and it is estimated in optical communication lines by different indirect methods, usually by employing the concept of the Q factor of the optical communication line [11]. In the case of the binary OOK format, by assuming that the statistics of zero and unit beats is described by the normal Gaussian law, this factor is

$$Q = \frac{\mu_1 - \mu_0}{\sigma_1 + \sigma_0},$$

where μ_i and σ_i $(i = 0, 1)$ are the mathematical expectation and the root-mean-square deviation for zero and unit beats, respectively.

Then,

$$\text{BER} = \frac{1}{2}\text{erfc}\left(\frac{Q}{\sqrt{2}}\right) \approx \frac{\exp(-Q^2/4)}{\sqrt{2\pi}Q}.$$

Here, erfc is the modified error function, and $Q \geqslant 6$ corresponds to the BER $\leqslant 10^{-9}$.

In this paper, we use the Q factor as the criterion for the signal-transmission quality and the range of the high-quality communication is defined as the distance for which $Q = 6$. The communication range was calculated by using pseudo-random sequences of lengths $(2^{10} - 1) - (2^{14} - 1)$ bit. The communication range was taken as the minimal distance among all possible frequency channels. In most calculations, five frequency channels were used with the 40-Gbit s^{-1} transmission per frequency channel (the bit interval duration was $T_b = 25$ ps), and the distance between adjacent channels was $\delta\nu = 100$ GHz. The 'on' state of a transmitter was simulated by Gaussian pulses of duration $(0.33-0.66)T_b$.

The Q factor for the $\pi/2$ AP RZ OOK format was estimated similarly because the phase modulation in this format contains no information.

In the case of the RZ DPSK formats, the calculation of the Q factor should be modified [12, 13]. For this purpose, we will determine it from the difference of the optical phases of a signal on a detector ($\Delta\Phi$, 0 and $\Delta\Phi$, π). In this case, by assuming the Gaussian noise statistics [12], we have

$$Q_{\Delta\Phi} = \frac{\pi}{\sigma_{\Delta\Phi,0} + \sigma_{\Delta\Phi,\pi}},$$

where $\sigma_{\Delta\Phi,0}$ and $\sigma_{\Delta\Phi,\pi}$ are the root-mean-square deviations of the phase difference for 0 and π, respectively.

Note that the factor $Q_{\Delta\Phi}$ is related to the BER by the expression [12]

$$\text{BER} = \text{erfc}\left(\frac{Q_{\Delta\Phi}}{\sqrt{2}}\right),$$

and $Q = 6.1$ corresponds to the BER $= 10^{-9}$. The $Q_{\Delta\Phi}$ factor for the $\pi/2$ RZ DPSK format is introduced similarly.

Let us introduce the alternative 'amplitude Q factor' (Q_A) defined by the expression

$$Q_A = \frac{\langle |A_n| \rangle}{\sigma_{|A_n|}},$$

where $|A_n|$ is the optical-field amplitude in front of a delay interferometer and n in the number of the bit interval. Then, in the case of the RZ DPSK formats, the BER and communication range are determined from the smallest of Q_A and $Q_{\Delta\Phi}$ factors.

When a particular configuration of a FOCL is studied by simulations, the problem of the line optimisation appears which involves the determination of its optimal parameters and the optical signal providing the maximum information capacity of the line. (The information capacity is the quantity $B_\Sigma L_D$, where L_D is the communication line range, which is determined from the specified BER.)

Consider now mathematical models that were used to describe fibre optical amplifiers: lumped erbium-doped fibre amplifiers (EDFAs) and forward- and backward-pumped Raman amplifiers (FRA and BRA).

In the case of EDFAs, the amplitude of an optical signal was multiplied by $\sqrt{G}$, where G is the gain of the amplifier. Spontaneous emission noise was described by the white noise model. The spectral density of the white noise was calculated from the expression

$$S_{\text{sp}} = (G - 1)n_{\text{sp}}h\nu_s,$$

where h is Planck's constant; ν_s is the carrier frequency of the signal; and n_{sp} is the spontaneous emission coefficient related to the noise factor (NF) of the amplifier by the expression

$$\text{NF} = \frac{2n_{\text{sp}}(G - 1)}{G}.$$

The noise factor of the EDFA is NF = 4.5 dB. Erbium-doped fibre amplifiers were used at the end of each periodic section (after a DCF). Optical signals in standard SMFs were amplified by using FRAs and (or) BRAs.

Raman amplification was simulated by using a system of ordinary differential equations for average signal and pump powers taking into account the ASE (amplified spontaneous emission) and backward Rayleigh scattering noises [14]. This model in the case of pumping at one wavelength had the form

$$\frac{dP_p^-}{dz} = \alpha_p P_p^- - \epsilon_p P_p^+ + \frac{\nu_p}{\nu_s}\frac{g_{ps}}{A_{\text{eff}}}\left\{P_s^+ + P_s^- + 4h\nu_s\Delta\nu_s \times \left[1 + \frac{1}{\exp[h(\nu_p - \nu_s)/kT] - 1}\right]\right\}P_p^-,$$

$$\frac{dP_p^+}{dz} = -\alpha_p P_p^+ + \epsilon_p P_p^- + \frac{\nu_p}{\nu_s}\frac{g_{ps}}{A_{\text{eff}}}\left\{P_s^+ + P_s^- + 4h\nu_s\Delta\nu_s \times\right.$$

$$\times\left[1+\frac{1}{\exp[h(\nu_p-\nu_s)/kT]-1}\right]\Bigg\}P_p^+,$$

$$\frac{dP_s^+}{dz}=-\alpha_s P_s^+ + \epsilon_s P_s^- + \frac{g_{ps}}{A_{eff}}(P_p^- + P_p^+)$$

$$\times\left\{P_s^+ + 2h\nu_s\Delta\nu_s\left[1+\frac{1}{\exp[h(\nu_p-\nu_s)/kT]-1}\right]\right\},$$

$$\frac{dP_s^-}{dz}=\alpha_s P_s^- - \epsilon_s P_s^+ - \frac{g_{ps}}{A_{eff}}(P_p^- + P_p^+)$$

$$\times\left\{P_s^- + 2h\nu_s\Delta\nu_s\left[1+\frac{1}{\exp[h(\nu_p-\nu_s)/kT]-1}\right]\right\},$$

where P_s^+ and P_s^- are the average powers of signals propagating at the central carrier frequency ν_s forward and backward, respectively; α_p and α_s are the absorption coefficients for the pump and signal; g_{ps}/A_{eff} is the ratio of the Raman gain to the effective mode area of the fibre; $\Delta\nu_s$ is the total frequency band of the signal propagation (the total frequency band for all frequency channels considered in calculations); ϵ_p and ϵ_s are the backward Rayleigh scattering coefficients at the pump and signal frequency, respectively.

The boundary conditions at the beginning ($z=0$) and the end ($z=L$) of the Raman gain interval are

$$P_p^-(L)=P_{p0}^-,\quad P_p^+(0)=P_{p0}^+,$$

$$P_s^+(0)=P_{s0},\quad P_s^-(L)=0.$$

If signal losses within this interval were completely compensated by the Raman gain, the natural boundary condition $P_s^+(L)=P_s^+(0)=P_{s0}$ was used. If the types of fibres were changed within the length L, the fibre splice losses were neglected. In the calculations presented below, $L=L_{SMF}$.

After solving the boundary-value problem for the initial system of equations, we calculate the coefficient

$$\alpha_s^{eff}(z)=\alpha_s-\frac{g_{ps}}{A_{eff}}\left[P_p^+(z)+P_p^-(z)\right]$$

and substitute $\alpha_s^{eff}(z)/2$ into (1) instead of the coefficient γ_s.

Let us rewrite the equation for the signal power P_s^+ in the form

$$\frac{dP_s^+}{dz}=-\left[\alpha_s+\frac{g_{ps}}{A_{eff}}\left(P_p^-+P_p^+\right)\right]P_s^+ + 2h\nu_s\Delta\nu_s$$

$$\times\left[1+\frac{1}{\exp[h(\nu_p-\nu_s)/kT]-1}\right]\frac{g_{ps}}{A_{eff}}\left(P_p^-+P_p^+\right)$$

$$+\epsilon_s P_s^- = -\alpha_s^{eff}(z)P_s^+ + S_1(z)+S_2(z),$$

where

$$S_1(z)=2h\nu_s\Delta\nu_s\left[1+\frac{1}{\exp[h(\nu_p-\nu_s)/kT]-1}\right]$$

$$\times\frac{g_{ps}}{A_{eff}}\left(P_p^-+P_p^+\right),\quad S_2(z)=\epsilon_s P_s^-.$$

To take into account the ASE noise, random complex quantities η_1 and η_2 are added to the optical signal amplitude, whose correlations give $S_1(z)$ and $S_2(z)$, respectively.

Note that all the parameters used in the paper correspond to real typical Raman and erbium-doped fibre amplifiers.

3. Results of mathematical simulation

We present below only the main results of massive numerical calculations on the optimisation of the transmission characteristics of a FOCL based on the modulation formats described above. Because a combined amplification scheme with erbium-doped fibre and Raman amplifiers is used in the dispersion configuration shown in Fig. 1, we introduce two parameters $\alpha=G_R/(G_R+G_E)$ and $\eta=G_B/(G_B+G_F)$. Here, G_R and G_E are the gains of Raman and erbium-doped fibre amplifiers, respectively, and G_B and G_F are the gains in Raman fibre amplifiers upon forward and backward pumping, respectively.

First of all, we compare the data-transmission efficiency in the optical communication line based on the RZ OOK and $\pi/2$ AP RZ OOK formats. The total length of one periodic section of this line was 100 km. We simulate below the propagation of Gaussian pulses with the FWHM $T_{0.5}=12.5$ ps (off-duty ratio is 50%).

Figure 3a shows isolines of the communication range in the plane of parameters (the average dispersion of the line is $\langle D\rangle$ and the average signal power is $\langle P\rangle$) for the $\pi/2$ AP RZ OOK format. The values of parameters η, α, and the widths of a rectangular optical fibre (B_{op}) and an electric third-order Butterworth filter (B_{el}) are indicated in the figure. Figure 3b shows the dependence of the communication range on the average power $\langle P\rangle$ of the optical signal for the optimal set of all other parameters. The solid and dashed curves correspond to the $\pi/2$ AP RZ OOK and RZ OOK

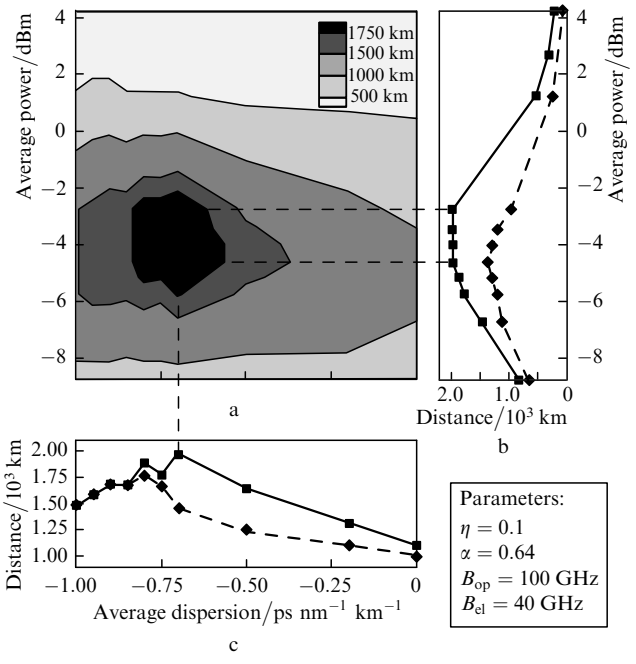

Figure 3. Communication-range isolines in the $\langle D\rangle$, $\langle P\rangle$ plane for the $\pi/2$ AP RZ OOK and RZ OOK formats.

formats, respectively. One can see that, although the use of the $\pi/2$ AP RZ OOK format provides only a small increase in the communication range compared to that in the case of the RZ OOK format (approximately by 200 km), the latter proves to be less stable to variations in $\langle D\rangle$ and $\langle P\rangle$. In addition, the optimal average power of a signal in the case of the $\pi/2$ AP RZ OOK format is higher by 2 dBm than that for the RZ OOK format. Note that this fact was experimentally confirmed (for another system) in paper [4].

Let us compare now the transmission characteristics of the RZ DPSK and $\pi/2$ RZ DPSK modulation formats (Fig. 4). Figure 4a presents the isolines of the communication range in the plane of parameters $\langle D\rangle$ and $\langle P\rangle$ for the $\pi/2$ RZ DPSK format, and Figure 4b shows the dependences of the communication range on the average signal power $\langle P\rangle$ for the optimal set of the rest of parameters. The solid and dashed curves correspond to the $\pi/2$ RZ DPSK and RZ DPSK formats, respectively. Figure 4c presents the dependences of the communication range on the average dispersion $\langle D\rangle$ of the line for these formats. One can see that the $\pi/2$ RZ DPSK format provides better transmission characteristics of the communication line in the range of average dispersions $\langle D\rangle = -0.35 \div -0.15$ ps nm^{-1} km^{-1} and average powers $\langle P\rangle = -8 \div -2$ dBm than the RZ DPSK format. The communication range increases approximately by a factor of one and a half, from 4680 km for the RZ DPSK format to 6680 km for the $\pi/2$ RZ DPSK format.

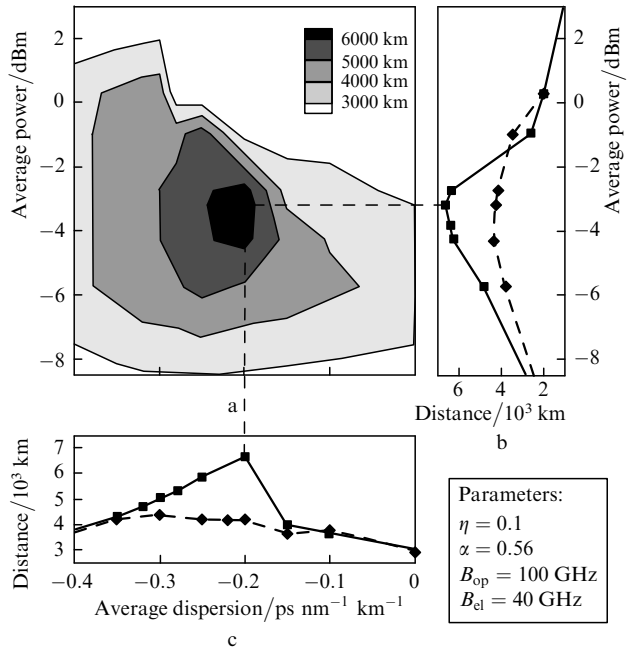

Figure 4. Communication-range isolines in the $\langle D\rangle$, $\langle P\rangle$ plane for the $\pi/2$ AP RZ OOK and RZ OOK formats.

The data-transmission efficiencies in the cases of using the $\pi/2$ AP RZ OOK and $\pi/2$ RZ OOK formats are compared in Fig. 5. Figure 5a shows the isolines of the communication range for the $\pi/2$ AP RZ OOK format (at the left) and the $\pi/2$ RZ DPSK format (at the right). Figure 5b presents the dependences of the communication range on the average power $\langle P\rangle$ for the $\pi/2$ RZ DPSK format (solid curve) and the $\pi/2$ AP RZ OOK format (dashed curve). Figure 5c shows the dependences of the communication range on the average dispersion $\langle D\rangle$. Note

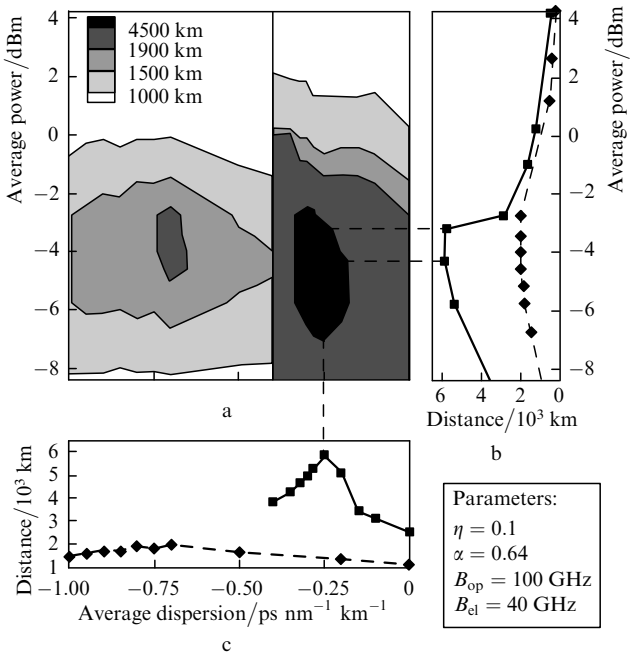

Figure 5. Communication-range isolines for the $\pi/2$ AP RZ OOK (at the left in Fig. 5a) and $\pi/2$ RZ DPSK (at the right in Fig. 5a) formats.

that the optimal propagation of a signal in the case of the $\pi/2$ AP RZ OOK format occurs for a considerably larger normal average dispersion than in the case of the $\pi/2$ RZ DPSK format.

Consider now the dependence of the communication range on the ratio of the Gaussian pulse duration $T_{0.5}$ to that of the bit interval $T_b = 25$ ps for the $\pi/2$ RZ DPSK format. Figure 6 shows the dependence of the communication range on the optimal average dispersion $\langle D\rangle_{opt}$ of a periodic section for a number of values of $T_{0.5}/T_b$, and Figure 7 demonstrates the dependence of the communication range on the optimal average power $\langle P\rangle_{opt}$ of the optical signal. One can see that the optimal average dispersion $\langle D\rangle_{opt}$ decreases with decreasing the duration of carrier Gaussian pulses. The dependence of the optimal average power on the pulse duration is more complicated.

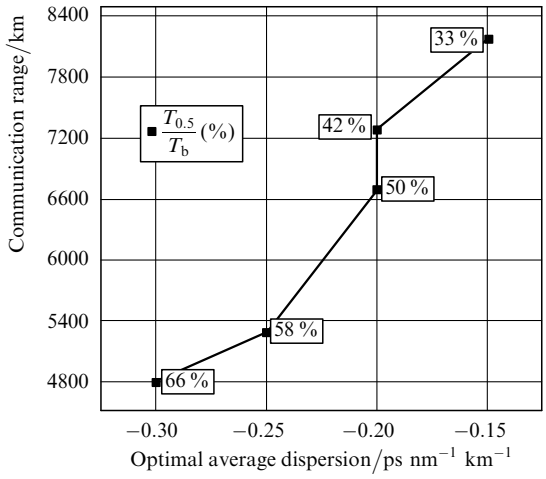

Figure 6. Dependence of the communication range on the optimal average dispersion of a periodic section for the $\pi/2$ RZ DPSK format.

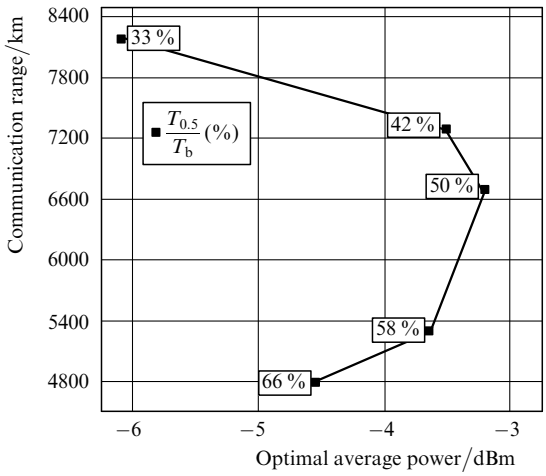

Figure 7. Dependence of the communication range on the optimal average power of an optical signal for the $\pi/2$ RZ DPSK format.

First it increases, achieving the maximum value for the carrier pulse duration $T_{0.5} = 0.5T_b$ (50 %), and then begins to decrease with increasing ratio $T_{0.5}/T_b$.

4. Conclusions

By using mathematical simulations, we have compared some modulation formats for data transmission in a high-bit-rate multichannel fibreoptic communication line with the dispersion control based on the combination of periodic sections made of a standard SMF with the positive group-velocity dispersion and a DCF with the compensated (negative) dispersion. The optimisation numerical calculations have shown that phase-modulated signals have a noticeable advantage over amplitude-modulated signals from the point of view of the communication range and the information capacity of fibreoptic communication lines.

We have obtained the following maximal communication ranges for different data-transmission formats for the carrier pulse duration $T_{0.5} = 0.5T_b$ (the off-duty ratio is 50%):

(i) RZ OOK format: $L_D = 1780$ km (transmission regime is realised for $\eta = 1$, $\alpha = 0.63$, $\langle P\rangle = -4.6$ dBm, $\langle D\rangle = -0.8$ ps nm^{-1} km^{-1}).

(ii) $\pi/2$ AP RZ OOK format: $L_D = 1980$ km ($\eta = 1$, $\alpha = 0.63$, $\langle P\rangle = -2.7$ dBm, $\langle D\rangle = -0.7$ ps nm^{-1} km^{-1}).

(iii) RZ DPSK format: $L_D = 4680$ km ($\eta = 1$, $\alpha = 0.64$, $\langle P\rangle = -4.3$ dBm, $\langle D\rangle = -0.3$ ps nm^{-1} km^{-1}).

(iv) $\pi/2$ RZ DPSK format: $L_D = 6680$ km ($\eta = 1$, $\alpha = 0.64$, $\langle P\rangle = -3.2$ dBm, $\langle D\rangle = -0.2$ ps nm^{-1} km^{-1}).

We have found that the communication range increases (for fixed requirements to the BER) with decreasing the carrier pulse duration.

It follows from the results of the paper that the maximal communication range at low-power signals is restricted by the additive accumulation of noises and for high-power signals – by nonlinear effects.

Acknowledgements. This study was supported by Integration Interdisciplinary Project No. 31, the Russian Ministry of Education (Grant No. 13-06-01), and INTAS (Grant No. 03-56-203).

References

1. Dianov E.M. *Vestnik RAS*, **70**, 1010 (2000).
2. Velichko M.A., Nanii O.E., Sus'yan A.A. *Lightwave Russ. Edit.*, (4), 21 (2005).
3. Agrawal G.P. *Applications of Nonlinear Fiber Optics* (New York: Acad. Press, 2001).
4. Gill D.M., Gnauck A.H., Liu X., Wei X., Su Y. *IEEE Photon. Tech. Lett.*, **16** (3), 906 (2004).
5. Gnauck A.H. et al. *Proc. OFC'2002* (Anaheim, CA, 2002) Postdeadline Paper FC2.
6. Zhu B. et al. *Proc. ECOC'2002* (Copenhagen, Denmark, 2002) Postdeadline paper PD4.2.
7. Bissessur H., Charlet G., Gohin E., Simonneau C., Pierre L., Idler W. *Proc. ECOC'2002* (Copenhagen, Denmark, 2002) paper 8.1.2.
8. Liu X., Wei X., Slusher R.E., McKinstrie C.J. *Opt. Lett*, **27**, 1616 (2002).
9. Wei X., Gnauck A.H., Gill D.M. *IEEE Photon. Tech. Lett.*, **15** (11), 1639 (2003).
10. Agrawal G.P. *Nonlinear Fiber Optics* (New York: Acad. Press, 2001).
11. Agrawal G.P. *Fiber-Optic Communication Systems* (New York: John Wiley&Sons, 1997).
12. Wei X., Liu X., Xu C. *IEEE Photon. Tech. Lett.*, **15** (11), 1636 (2003).
13. Xu C., Liu X., Wei X. *IEEE J. Sel. Top. Quantum Electron.*, **10** (2), 281 (2004).
14. Kidorf H. et al. *IEEE Photon. Tech. Lett.*, **11**, 530 (1999).